



HAL
open science

Three phase PV inverter LCOE optimization considering technological choice

Morteza Tadbiri Nooshabadi, Jean-Luc Schanen, Shahrokh Farhangi, Hossein
Iman-Eini

► **To cite this version:**

Morteza Tadbiri Nooshabadi, Jean-Luc Schanen, Shahrokh Farhangi, Hossein Iman-Eini. Three phase PV inverter LCOE optimization considering technological choice. EPE 2022 : 24th European Conference on Power Electronics and Applications, Sep 2022, Hannovre, Germany. hal-03779376

HAL Id: hal-03779376

<https://hal.science/hal-03779376>

Submitted on 16 Sep 2022

HAL is a multi-disciplinary open access archive for the deposit and dissemination of scientific research documents, whether they are published or not. The documents may come from teaching and research institutions in France or abroad, or from public or private research centers.

L'archive ouverte pluridisciplinaire **HAL**, est destinée au dépôt et à la diffusion de documents scientifiques de niveau recherche, publiés ou non, émanant des établissements d'enseignement et de recherche français ou étrangers, des laboratoires publics ou privés.

Three phase PV inverter LCOE optimization considering technological choice

Morteza Tadbiri Nooshabadi^{1,2}, Jean-Luc Schanen¹, Shahrokh Farhangi², Hossein Iman-Eini²

¹Univ. Grenoble Alpes, CNRS,

Grenoble INP, G2Elab,

38000 Grenoble, France

jean-luc.schanen@grenoble-inp.fr

²University of Tehran

School of Electrical and Computer Engineering

Tehran, Iran

m.tadbiri@ut.ac.ir, Imaneini@ut.ac.ir

Abstract

This work uses design by optimization of power electronics converter to achieve the best Levelized Cost of Energy in a PV application. The methodology uses detailed models of power electronics active and passive components to determine the cost and performances of the solid-state energy conversion, and connect them to the system level vision. The deterministic algorithm used for converter sizing allows taking into account a large number of variables and constraints. Methodology, models and some illustrations of the results are provided in this paper.

Keywords

«Design optimization», «Photovoltaic», «Levelized cost of energy», «Reliability», «Cost analysis»

I. Introduction

Photovoltaic (PV) technology requests a high efficiency power conversion in order to achieve acceptable price per produced kWh. Indeed the cost of power converters is not negligible in the installation. Both cost and performances of the power electronics conversion depends on the choice of components and the converter sizing: for instance, SiC devices are more expensive than Si IGBTs, but exhibit lower losses. The choice is therefore not straightforward. On the other hand, it is well known that the efficiency of a power converter depends on its nominal power [1], as well as its cost. Therefore, the design of a converter and the associated components ratings becomes a crucial issue.

In order to quantify and compare the cost for different energy technologies, Levelized Cost of Energy (LCOE) index is generally used [2]. LCOE represents the price at which the electricity is generated from a specific energy source over the whole lifetime of the generation unit. The index is expressed by:

$$LCOE = \frac{\text{Total life cycle cost}}{\text{Total lifetime energy production}} \quad (1)$$

Based on above expression, a cost-effective grid-connected PV systems can be obtained by minimizing the initial investment cost which is included the cost of the PV system components (e.g., PV modules, DC/AC inverters, etc.), maximizing the amount of energy injected into the grid, and increasing its reliability. The lifetime of the PV system components are indeed very important since any failure in operational time causes missing PV energy [3]. The injected energy into the grid is upped by maximum power point tracker (MPPT) control algorithm [4].

The rule of thumb for solar inverter overclocking is that solar panel capacity should not be more than roughly 30% greater than inverter capacity. More scientific work has already been done on optimal sizing of PV inverters, using various models and algorithms [5]. On the modeling point of view, database of existing inverters, simulations or simple analytical models have been reported [5-6]. Obviously, the mission profile (irradiation, local climate [7]) is always taken into account in these kinds of studies.

However, converter-level analytical models are only representative of a global behavior, and cannot reflect precisely the impact of technological choice and component design. Database of existing hardware

is by definition limited to available technologies and cannot be used to investigate potential breakthrough or unconventional design. Precise simulation of the power electronics converter can of course be used to obtain the performances depending on the technological choices and inverter design, but it is very long and not really compatible with optimization, especially if various technological or structural options are considered.

Therefore, this paper proposes a methodology which is clearly optimization-oriented, based on component models to obtain the minimum Levelized Cost of Energy (LCOE) of the power electronics part only. Each part of the PV inverter and MPPT boost converter are considered, and the global performances of the conversion take therefore into account the components behavior and sizing. Several constraints are addressed in the optimization: device-level constraints (as the semiconductor maximum temperature), as well as system level constraints (as THD on the AC side). Section II will illustrate the interest of having a precise representation of the converters performances, based on a case study using three different manufacturers. Section III will then provide all models used in the converters optimization, as well as the optimization methodology, which is based on a deterministic algorithm. The lifetime prediction is also evaluated in this section. Section IV will present some optimization results for various cases.

II. LCOE of industrial inverters: case study

The evaluation of the performances of a PV inverter has to be achieved with respect to the balance between the investment cost (price of the inverter if we focus on this part of the PV system only) and the amount of energy produced in the product lifetime. In order to quantify and compare the cost for different situations, the Levelized Cost of Energy (LCOE) index will be used for the converters. For this purpose, the mission profile of the PV inverter has first to be defined, and the efficiency of the inverter vs power to be considered. Fig. 2 shows three cases studies of the same power (20kVA) obtained from manufacturer datasheets [8-10]. To enlarge the study, two different locations were considered (Grenoble (France) and Tehran (Iran)), with different irradiation characteristics.

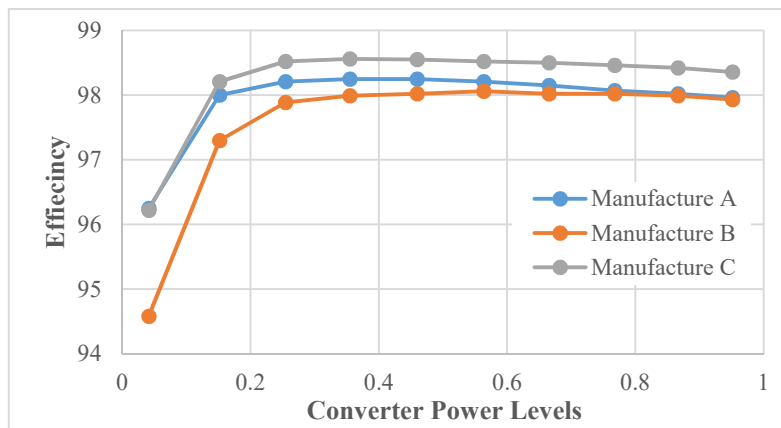


Fig. 2: The inverter efficiency curve for 3 different 20 kVA inverters

The mission profile was developed based on local measurements. Data points were taken every ten minutes, corresponding to the 10-minutes average of irradiance and ambient temperature. The mean daily profiles, averaged over the duration of the considered data in Grenoble, are shown in Fig 3. It was then split into 10 steps for operational phases and one step for dormant phase (Fig. 4), for an example of application which is a 20 kW installation, composed of 4 strings of 16 * 320W panels (Fig. 5). By using [11] method, Table.1 shows the mission profile data at Grenoble in each step.

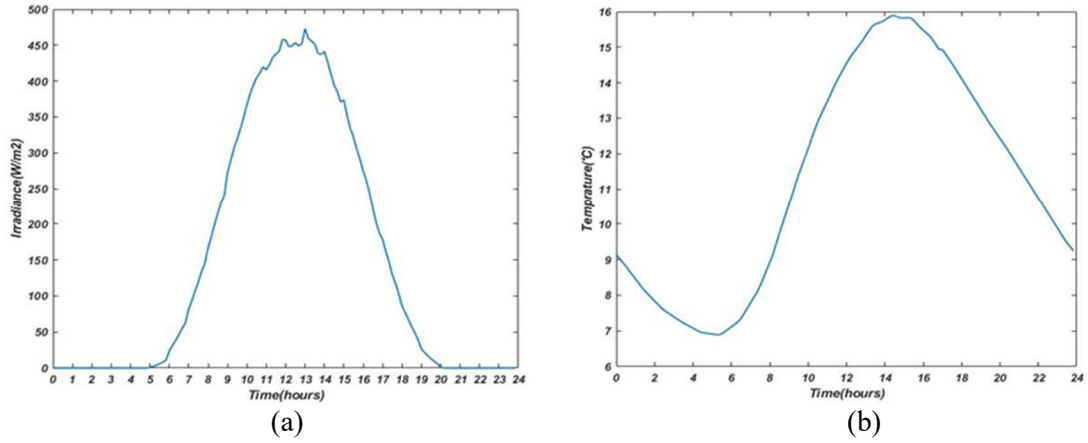


Fig. 3: Mean diurnal profiles in Grenoble. (a) Irradiance, (b) Temperature.

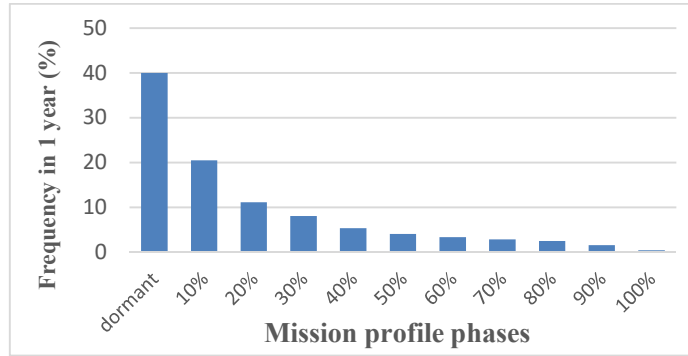


Fig. 4: Mission profile expressed in 10 different phases. Percent length of each phase, at location Grenoble

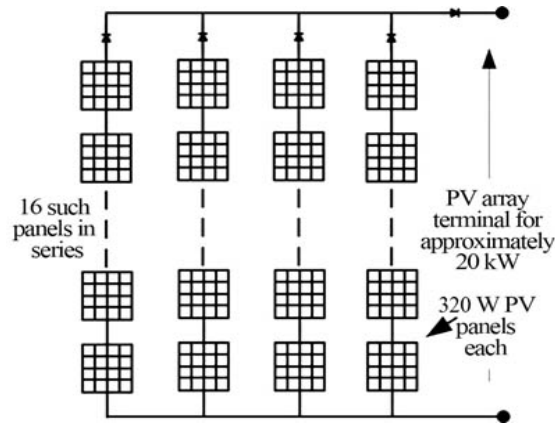


Fig. 5: PV panel arrangement to make it an array of 20 kW.

TABLE I: GRENOBLE MISSION PROFILE

	Phase	hL(hour)	TL(°C)	V _{pv}	P _{pv}
P _{max} = 20.533 kW	dormant	3503.667	10.35695	0	0
	10%	1796.333	11.53196	610.10	823.28
	20%	974.6667	13.44483	639.32	3031.9
	30%	708.3333	15.28658	641.26	5088.7
	40%	468.1667	17.10864	638.29	7095.6
	50%	359.8333	18.66902	632.91	9194.6
	60%	295.1667	19.83923	628.72	11270
	70%	253.8333	20.89177	623.22	13305
	80%	222.6667	21.70667	618.04	15351
	90%	136.8333	22.02976	613.16	17328
	100%	40.5	22.07141	611.07	19017

By combining the mission profile data with the efficiency curve of inverter, the total amount of energy is obtained as eq. (2), for a duration of 25 year as follow (this duration is considered as useful lifetime of solar panel and industrial inverters are guaranteed by manufactures to work without any problem in this time duration).

$$E(MWh) = 25 \text{ yr} * \sum_{i=1}^{10} P_{PV_i}(W) \cdot \eta_i \cdot t_i(h) \cdot 10^{-6} \quad (2)$$

Referring to the price of each inverter [12] leads to the LCOE of each inverter, in €/MWh (Fig.6). From this figure, it is clear that the efficiency difference (Fig. 2), which is due to different technological and design choices, clearly impacts the LCOE. Regardless the inverter lifetime, which will be addressed in section III of the paper, manufacture C inverter seems to be best choice from an LCOE perspective.

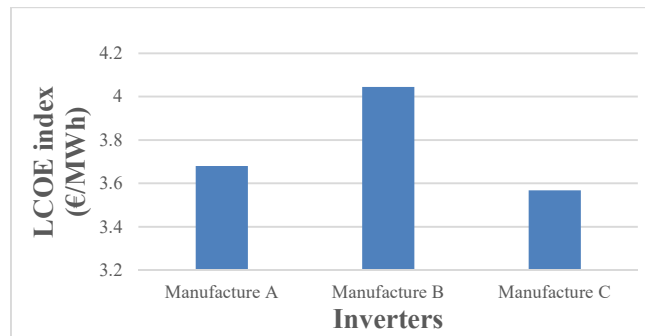


Fig. 6: The LCOE index in each inverter for location Grenoble.

Another study case consists in choosing various sizing powers from the same manufacturer (Manufacture C inverters in this case). By applying the mission profile to each of them, the efficiency curves (Fig.7) and finally the LCOEs are obtained. The usual PV panel degradation [13] has not be considered here for simplicity. Results, shown in Fig. 8 for location Tehran, show that a 17kW sizing is the best. The same approach for localization Grenoble shows that a 12kW choice would be better, according to LCOE index applied to the inverter. That is notable that there is a PV array oversizing in inverters with nominal power less than 20 kW which causes to some of PV energy produced by panels have been lost and, in this condition, inverter works in its nominal power. Even though some of PV energy have been lost, this method is used to gain more energy during the low solar irradiance [3]. So, the LCOE index shows the best choice for inverter in a fixed installed PV array condition.

This simple illustration on existing PV inverters shows that both technological choice and converter design impact the LCOE, and have to be considered when installing a PV inverter in a given location.

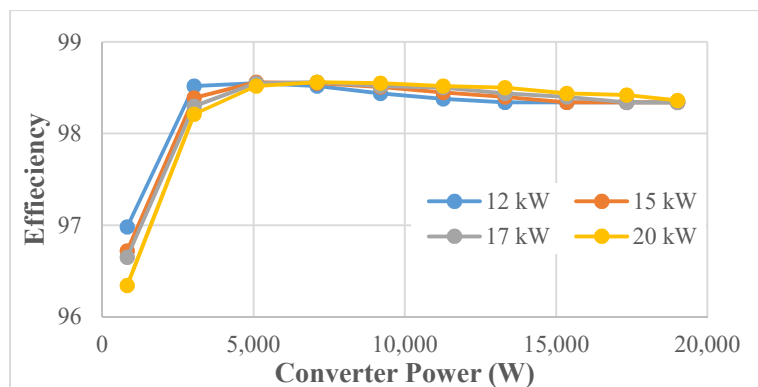


Fig. 7: Efficiency curves for four different power levels

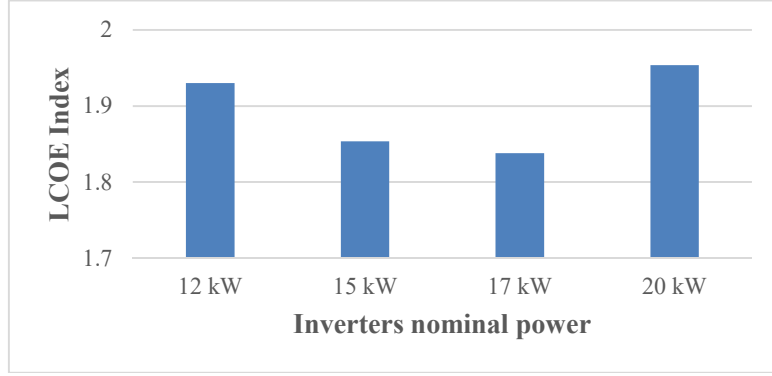


Fig. 8: LCOE index for manufacture C inverters at location Tehran

As mentioned before, lifetime is a mandatory part of LCOE calculation, and has not been included in the previous study, since no information is provided in commercial inverters catalogs. For obtaining the previous results, it was assumed that each inverter was working at least 25 years, based on manufacturer claiming. However, lifetime evaluation needs a comprehensive knowledge on inverter components. This will be obtained through a detailed analysis of the converter design, using simple but quite accurate models for pre-design. This pre-design step will also allow evaluating the inverter cost, based on the bill of materials (BoM). The next section will illustrate all models used for inverter pre-design.

III. Models for inverter pre-sizing

Fig. 9 shows the hardware components of a PV-System from the solar array to the grid. The grid-connected photovoltaic system has two main parts: the maximum power point tracker (MPPT) and the grid-connected inverter. The MPPT is responsible for maintaining the solar array at its maximum power as well as supplying the DC link voltage in the specified value. The inverter connected to the grid is responsible for supplying the sine current injected to the grid according to the existing standards, what leads to the necessity of output filters L_1 -C- L_2 . Each component of the two converters (active and passive) are modeled quite accurately.

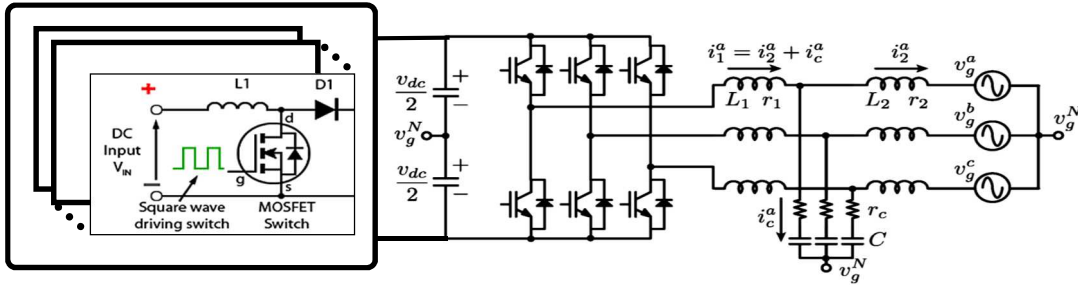


Fig. 9: Different components of the grid-connected photovoltaic system

A. AC Filter

In case of PWM inverters, the design of the AC inductor is particularly critical, as it concentrates a large part of losses of the whole system [14]. This inductor should have a significant value to decrease the ripple at switching frequency, but should also fulfill a thermal constraint. The saturation phenomenon may decrease the inductor value during the current peak and affect the effectiveness of the filter. Therefore, it is taken into account. Design procedure of inductor and LC filter with saturation consideration is explained in [15] and has been adapted to LCL filter. It considers the material choice, the core and wiring size. The capacitors are designed according to the needed capacitance, voltage and RMS current. To do this, the ripple current is assumed to be sinusoidal, at the switching frequency, and centered on the low frequency current. These assumptions are translated into eq. (3) as follows:

$$I_{L1,AC}(t) = i_1 + i_{ripple} = \sqrt{2}I_{L1,AC} \sin(\omega t + \varphi_1) + \frac{\Delta I_{L1,AC}(t)}{2} \sin(\omega_{sw} t) \quad (3)$$

$\Delta I_{L1,AC}(t)$ is the current ripple in the inductor at the inverter side that is variable due to the saturation effect. Thus, for simplicity, a mean ripple is defined:

$$\Delta I_{L1,AC,mean} = \frac{1}{N_p} \sum_i^{N_p} \Delta I_{L1,AC}(t_i) \quad (4)$$

The ripple currents in L_2 and C obtain by putting L_1 ripple current in filter transfer function as follows:

$$\Delta I_{L2,AC}(t) = \left| \frac{r_c + \frac{1}{j\omega_{sw}C}}{R_f + \frac{1}{j\omega_{sw}C} + j\omega_{sw}L_2} \right| \Delta I_{L1,AC}(t) \quad (5)$$

$$\Delta I_{C_f,AC}(t) = \left| \frac{j\omega_{sw}L_2}{R_f + \frac{1}{j\omega_{sw}C} + j\omega_{sw}L_2} \right| \Delta I_{L1,AC}(t) \quad (6)$$

Therefore, knowing the filter parameters, the other steps of [15] can be continued. Also, the THD of injected current that should be limited in standard margin, is calculated by:

$$THD = 100 \frac{\frac{\Delta I_{L2,AC,mean}}{2\sqrt{2}}}{I_{L2,AC}} \quad (7)$$

B. Inverter Losses

A bipolar PWM pulse, computed by a comparison of a sine-wave and a triangular carrier, controls the commutation of the switches. The power losses in the inverter depend on the current and voltage patterns across the switches and on the switches sizing (i.e. voltage and current rating), which is also a design parameter. Indeed, higher current capability leads to reduced conduction losses but increased switching losses. In accordance with [16], the RMS and average current flowing through each branch of inverter is analytically calculated by computing switching angles. This calculation takes into account the AC current ripple, which depends on the AC output filter. Losses in inverter are calculated by [17]. The switching frequency is also a design variable. As in [17], the losses are stated based on pure sine current, in order to consider the ripple current in calculations, the ripple current in summing in fundamental current as below:

$$i(t) = \sqrt{I_{m1}^2 + \frac{\Delta I_{L1,AC,mean}^2}{4}} \sin(\omega t + \varphi_i) \quad (8)$$

In switching losses, the switch turns on in $i_1 - \frac{\Delta I_{L1,AC,mean}}{2}$ current and turns off in $i_1 + \frac{\Delta I_{L1,AC,mean}}{2}$ current. Also, the diode turns off in $i_1 - \frac{\Delta I_{L1,AC,mean}}{2}$ current. Therefore, energy losses in the MOSFET and diode are modified as below:

$$E_{on} = E_{on} \left(V_{dc}, i_1 - \frac{\Delta I_{L1,AC,mean}}{2} \right) \quad (9)$$

$$E_{off} = E_{off} \left(V_{dc}, i_1 + \frac{\Delta I_{L1,AC,mean}}{2} \right) \quad (10)$$

$$E_{d(off)} = E_{d(off)} \left(V_{dc}, i_1 - \frac{\Delta I_{L1,AC,mean}}{2} \right) \quad (11)$$

C. Boost Converter

Boost converter is composed of inductor and switches. By using the same method as in previous sections in inductor design and also the switch current calculation, the output spectrum of current in boost converter is calculated. In the purpose of boost inductor waveform modeling, like as the current in AC filter, the ripple current is assumed to be sinusoidal at the switching frequency and superimposed on the dc part current. These assumptions are translated into eq. (12).

$$I_{Lb}(t) = I_{in} + \frac{\Delta I_{Lb}}{2} \sin(\omega_{sw,b} t) \quad (12)$$

The comparison between the modeled L_b current and the simulation result is shown in Fig. 10.

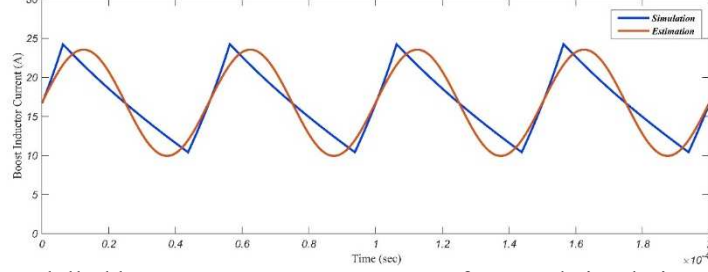


Fig. 10: Modelled boost converter current waveform and simulation validation

Beside of current waveforms, the losses in inductor and switches are calculated. The switching frequency is again a design variable, as well as the semiconductor sizing. In the same way, by considering current as a ramp, the switch turns on in $I_{in} - \frac{\Delta I_{Lb}}{2}$ current and turns off in $I_{in} + \frac{\Delta I_{Lb}}{2}$ current. Also, the diode turns off in $I_{in} - \frac{\Delta I_{Lb}}{2}$ current. Therefore, energy losses in the switch and diode are calculated as inverter losses.

D. DC-link Capacitor

DC-link capacitor is designed based on the maximum allowed ripple voltage, but also on the maximum RMS current passing through the capacitor. This current is defined in the frequency domain by $i_c = i_{boost} - i_{inv}$ of the inverter input current i_{inv} and the output current i_{boost} of the boost converter which are obtained in previous steps. The steps for calculating the RMS current of the DC-link are explained in [16] and [18].

E. Thermal Model

Beside of dynamic and impedance modelling mentioned in [19], since the studying is based on steady-state conditions, the system is modeled by the thermal resistance (R_{th}). Junction temperature of switches and diodes are calculated based on thermal resistance from junction to ambient, and limited by constraints. By supposing that all of semiconductors are located on a unique heat-sink, the thermal model of the case studied photovoltaic inverter is shown in Fig. 11. Each loss is evaluated from sections B and C. The thermal resistances are evaluated according to a low power MOSFET and diode as reference semiconductors which can be paralleled by N_{sw} and N_d . In this case, the equivalent thermal resistance is calculated by dividing the reference value by the number of parallels semiconductors.

$$R_{th,eq,MOSFET(diode)} = R_{th,MOSFET(diode),ref} / N_{sw(diode)} \quad (13)$$

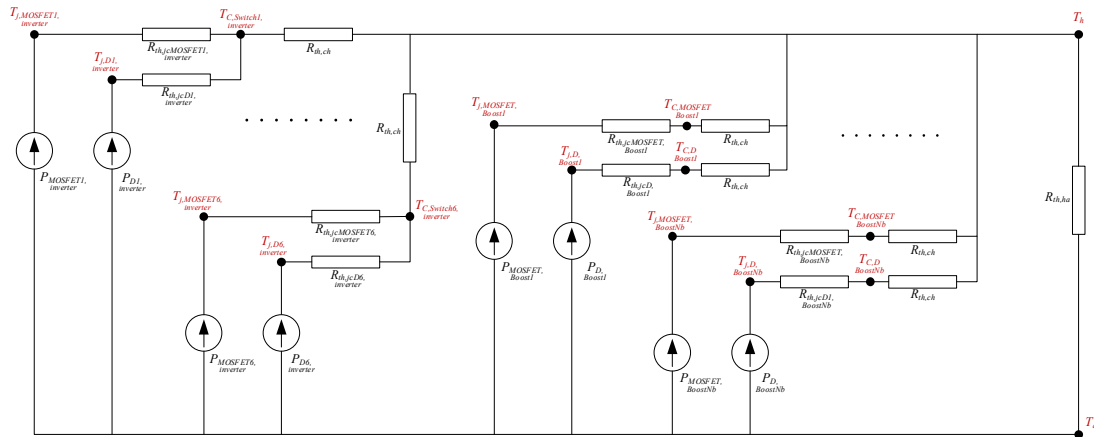


Fig. 11: Thermal model of the case studied photovoltaic inverter.

Using the thermal model of Fig. 11 allows evaluating the temperatures of each device, being the input of reliability models. Furthermore, the maximum allowed temperature is the sizing constraint for the heatsink.

F. Heatsink model

The heatsink is studied from the data of the [20] which has a large range of heatsinks in its productions. Fig. 12 shows the interpolation of a large amount of different heatsinks.

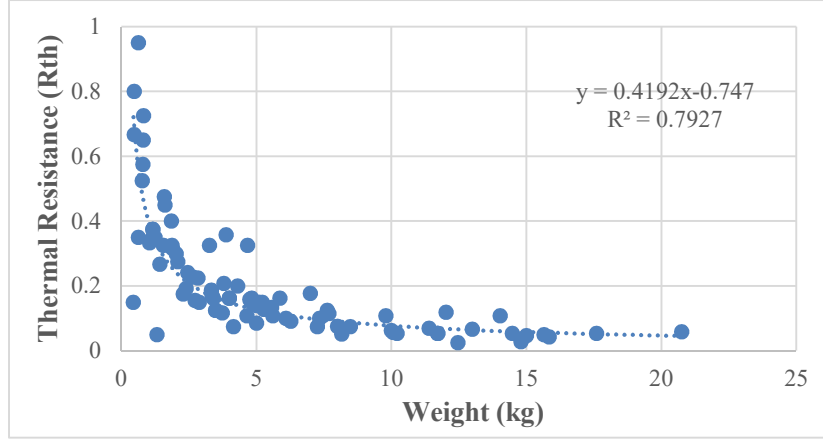


Fig. 12: Thermal resistance of the heatsink according to its weight

The thermal resistance parameter of the heatsink is expressed by its weight according to eq. 14.

$$Rth_{hs} = 0.4192W_{hs}^{-0.747} \quad (134)$$

G. Reliability Model

In order to obtain longer operational lifetime, the most fragile components must be specified, and reliability evaluation methodologies can be used for this approach. For this approach, FIDES methodology is used which is based on Physics-of-Failure (PoF) and developed by a French companies consortium. FIDES Methodology is supported by the analysis of test data, field returns and existing modelling. According to a previous evaluation, the FIDES methodology provides better results in compare with the observed ones [11]. FIDES is a standard which defines mathematical formula for evaluating the life-time of devices as a function of various parameters like as such as operating temperature, voltage and also manufacturing and mechanical stress [21]. Nevertheless, the most significant parameter in reliability and life-time evaluating is temperature of devices. Following the steps in [21] to evaluate the failure rate of each component in each phase of operation (λ_i^{phj}), and then each component failure rate (λ_i), the overall system failure rate is obtained by multiplying the failure rate of each component as follows:

$$\lambda_{total} = \prod_i \lambda_i \quad (15)$$

H. Cost Model

Despite the poor availability of cost data in academia, cost models are very difficult to establish, therefore, only the individual cost of components (semiconductors, capacitors, core and windings for inductors), based on manufacturer prices for large ordering quantities, numerical values for the cost model parameters are taken account. Of course, this is not representative of the actual cost of a PV inverter, but it is sufficient for comparison purpose. In addition to the analysis of the cost of components in the markets, it can be considered by the models that are proposed in [22].

IV. LCOE estimation for various case study

All previous models have been developed taking care to their derivability, in order to be used with a deterministic algorithm (Sequential Quadratic Programming method (SQP) [23]). This presents the advantage of being very effective in finding quickly the optimum in a large space of solution, with large amount of variable and constraints. The model indeed is composed of more than 25 parameters and 50 constraints (at component or system level). The design framework used is able to perform automatically the derivation of all equations, what leads to a significant time saving. The objective function is to reach the minimum cost for a given sizing power. In optimization process, the reliability is force to be at least more than 25 years to be insured that the inverter could work in PV panels lifetime. For each optimized inverter, the mission profile is applied. Of course, the maximum power is limited to the sizing power

during operation. To be noticed that overload capability has not be considered since the models cannot handle the consequence of this kind of overloads. Consequently, the converter is exactly sized regarding nominal power, without any margin. Fig. 13 shows the design level of optimization procedure where the design variables in each iteration are chosen. More than 25 variables are considered including filter parameters (core size and turn number for inductors), switching frequencies (inverter and boost converters), number of switches and The set of design variable should satisfy some constraints on THD, junction temperature of switches and diodes and rise temperature in capacitors. then, the LCOE index is evaluated by combining results of sections G and H and then the best set of design variables choose. The flowchart of LCOE optimization is presented in Fig. 14.

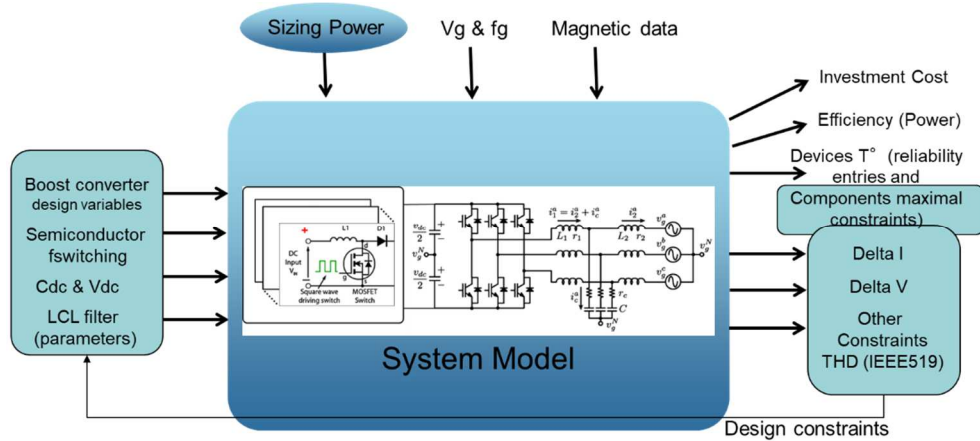


Fig. 13: the design level of optimization procedure with considering design variables as input.

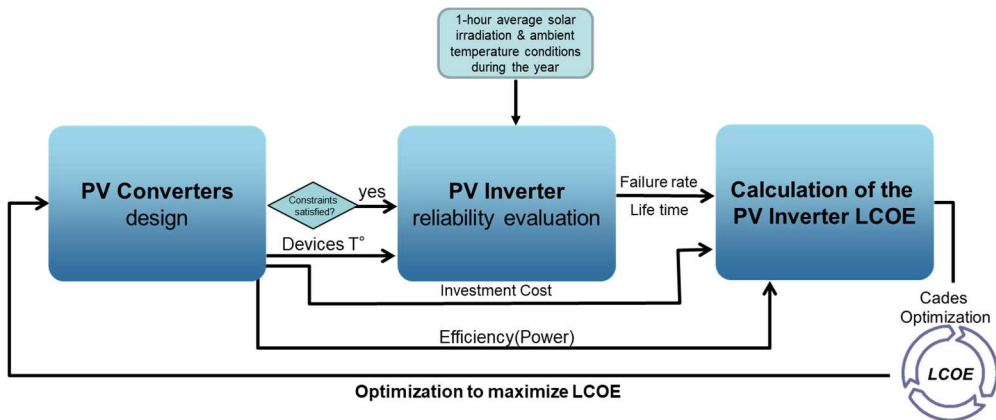


Fig. 14: The flowchart of LCOE optimization.

Results of LCOE for Grenoble and Tehran are displayed in Fig. 15. It is worth noting that the optimal sizing power is different for the two locations, according to the different solar irradiation. This confirms the results from previous work, which showed the interest of downsizing the nominal power to gain more energy yield during the low solar irradiance conditions [3]. Note that the LCOE index is applied to inverter only, and that the inverter cost is reduced to the sum of components cost, therefore absolute values of sizing power are not to be considered as a strict result, but only for comparison purpose (see conclusion).

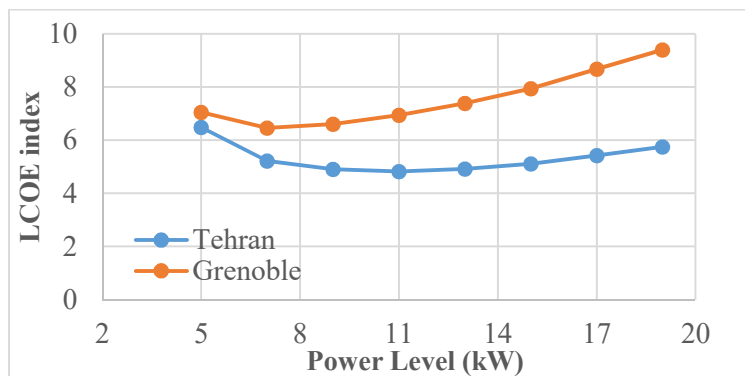


Fig. 15: LCOE index comparison for Grenoble and Tehran

Another interest of the approach is that it allows investigating the impact of some technological choices. For instance, using SiC MOSFET or Si IGBT has been illustrated in Fig 16, for location Tehran. It is worth noting that IGBT, despite is lower cost leads to higher LCOE. Indeed, its higher switching losses lead to reduced switching frequency (16 kHz roughly for each design, which was the minimum imposed for audition limit), what leads to higher cost for passive components, specifically to meet the THD constraint.

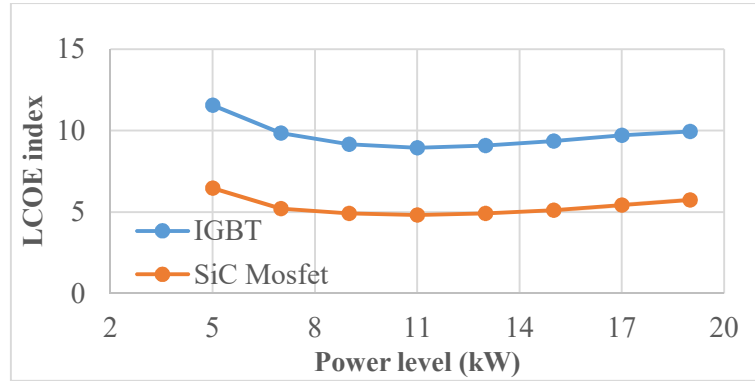


Fig. 16: LCOE index Si vs SiC (Tehran)

Another technological choice that can be considered is the comparison of the wire material between copper and aluminum. The LCOE index for both material is presented in Fig. 17 where this index is almost the same for both cases while the aluminum is cheaper than copper in the markets but the resistivity coefficient of aluminum (ρ) is higher than that of copper [24] and it causes more power losses in the system. Thus, the injected energy is lower than the other case. It should be noted that the temperature coefficient (α) is not considered in this study and since this coefficient is higher in aluminum than in copper the LCOE can be expected to be higher than the one presented.

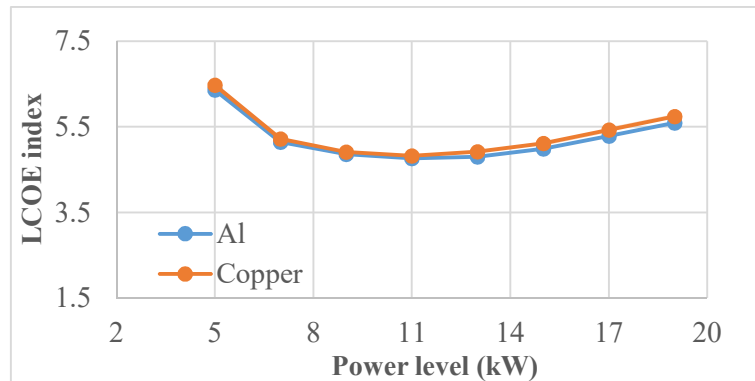


Fig. 17: LCOE index Copper vs Aluminium (Tehran)

V. Conclusions

Considering the actual sizing and technological choice for PV inverters is determining to solve the tradeoff between inverter cost and its performances during its lifetime. This paper illustrates first the impact of these parameters with existing inverters, using the LCOE index (applied to power electronics only). Then an optimization method is proposed, using detailed models of components, in order to obtain the best sizing power for the inverter, according to LCOE index and a given mission profile. The design method accounts for components and system level constraints. It is also applied to investigate the impact of semiconductor and material choice.

References

- [1] L. Keller and P. Affolter, "Optimizing the panel area of a photovoltaic system in relation to the static inverterU° practical results," *Solar Energy*, vol. 55, no. 1, pp. 1–7, 1995.
- [2] E. Koutroulis and F. Blaabjerg, "Design Optimization of Transformerless Grid-Connected PV Inverters Including Reliability," in *IEEE Transactions on Power Electronics*, vol. 28, no. 1, pp. 325-335, Jan. 2013, doi: 10.1109/TPEL.2012.2198670.

- [3] A. Sangwongwanich, Y. Yang, D. Sera, and F. Blaabjerg, "Mission Profile-Oriented Control for Reliability and Lifetime of Photovoltaic Inverters," 2018 Int. Power Electron. Conf. IPEC-Niigata - ECCE Asia 2018, pp. 2512–2518, 2018, doi: 10.23919/IPEC.2018.8507577.
- [4] R. Kadri, J.-P. Gaubert, and G. Champenois, "An improved maximum power point tracking for photovoltaic grid-connected inverter based on voltage-oriented control," *IEEE Trans. Ind. Electron.*, vol. 58, no. 1, pp. 66–75, Jan. 2011.
- [5] R. Nasiri, M. Khayamy, M. Rashidi, A. Nasiri and V. Bhavaraju, "Optimal Solar PV Sizing for Inverters Based on Specific Local Climate," 2018 IEEE Energy Conversion Congress and Exposition (ECCE), Portland, OR.
- [6] G. Velasco, F. Guinjoan, R. Pique, A. Conesa and J. J. Negroni, "Inverter Power Sizing Considerations in Grid-Connected PV Systems," 2007 European Conference on Power Electronics and Applications, Aalborg,
- [7] M.G.Kratzenberg, E.M.Deschamps, L.Nascimento, R.Rüther, H.H.Zürn, "Optimal Photovoltaic Inverter Sizing Considering Different Climate Conditions and Energy Prices",*Energy Procedia*, Volume 57, 2014, Pp 226-234
- [8] S. M. A. Solar and T. Ag, "Integrated service for ease and comfort," pp. 8–11.
- [9] Fronius, "Fronius Symo Datasheet," pp. 6–11, [Online]. Available: <http://www.fronius.com/>.
- [10] Huawei, "Smart String Inverter," pp. 2–3, 2019.
- [11] S. E. De Leon-Aldaco, H. Calleja, and J. Aguayo Alquicira, "Reliability and mission profiles of photovoltaic systems: A FIDES approach," *IEEE Trans. Power Electron.*, vol. 30, no. 5, pp. 2578–2586, 2015, doi: 10.1109/TPEL.2014.2356434.
- [12] "Solar inverters | Solar Inverter for PV System | Europe Solar Store." [Online]. Available: https://www.europe-solarstore.com/solar-inverters.html?inverter_power=24.
- [13] A. Sangwongwanich, Y. Yang, D. Sera, F. Blaabjerg, "Lifetime Evaluation of Grid-Connected PV Inverters Considering Panel Degradation Rates and Installation Sites," *IEEE Trans. Pow. Electr.*, vol. 33, no. 2, 2018.
- [14] T. Orłowska-Kowalska and M. Kaminski, *Advanced and Intelligent Control in Power Electronics and Drives*, vol. 531. 2014.
- [15] A. Voldoire, J. L. Schanen, J. P. Ferrieux, C. Gautier, C. Saber, "Optimal Design of an AC Filtering Inductor for a 3-Phase PWM Inverter Including Saturation Effect," *PEDSTC 2019*, Shiraz, Iran
- [16] A. Voldoire, J. L. Schanen, J. P. Ferrieux, C. Gautier, and C. Saber, "Analytical calculation of dc-link current for N-Interleaved 3-Phase PWM inverters considering AC current ripple," 2019 21st Eur. Conf. Power Electron. Appl. EPE 2019 ECCE Eur., p. P.1-P.10, 2019, doi: 10.23919/EPE.2019.8915183.
- [17] M. H. Ahmed, M. Wang, M. A. S. Hassan, and I. Ullah, "Power Loss Model and Efficiency Analysis of Three-Phase Inverter Based on SiC MOSFETs for PV Applications," *IEEE Access*, vol. 7, pp. 75768–75781, 2019.
- [18] J. W. Kolar and S. D. Round, "Analytical calculation of the RMS current stress on the DC-link capacitor of voltage-PWM converter systems," *IEE Proceedings - Electric Power Applications*, vol. 153, no. 4, p. 535, 2006, doi: 10.1049/ip-epa:20050458.
- [19] Y. Shen, S. Song, H. Wang, and F. Blaabjerg, "Cost-Volume-Reliability Pareto Optimization of a Photovoltaic Microinverter," in 2019 IEEE Applied Power Electronics Conference and Exposition (APEC), Mar. 2019, pp. 139–146. doi: 10.1109/APEC.2019.8722043.
- [20] "Wakefield Thermal Air Cooled Thermal Extrusions." <https://wakefieldthermal.com/thermal-solutions/air-cooled/thermal-extrusions/>
- [21] "FIDES guide 2009. Edition A. Reliability Methodology for Electronic Systems," 2010. [Online]. Available: www.fides-reliability.org.
- [22] R. Burkart and J. W. Kolar, "Component cost models for multi-objective optimizations of switched-mode power converters," in 2013 IEEE Energy Conversion Congress and Exposition, Sep. 2013, pp. 2139–2146.
- [23] P. T. Boggs and J. W. Tolle, "Sequential Quadratic Programming," *Acta Numer.*, vol. 4, pp. 1–51, 1995
- [24] Giancoli, Douglas C., *Physics*, 4th Ed, Prentice Hall, (1995).